Brownian Dynamics Study of Polymer Conformational Transitions‡

Eugene Helfand,* Z. R. Wasserman, and Thomas A. Weber

Bell Laboratories, Murray Hill, New Jersey 07974. *Received November 30, 1979*

ABSTRACT: The kinetics of conformational transitions in polymer molecules has been studied by performing a Brownian dynamics simulation. Rates are determined by compilation of first passage times and hazard analysis. The activation energy from an Arrhenius plot is slightly more than the barrier height separating the trans and gauche state. Some cooperativity of transitions on second neighbor bonds is noted, especially when these bonds are separated by a trans. Results are discussed in relation to a recent theory.

Conformational transitions from one rotational isomeric state to another are fundamental to rapid relaxation processes in polymers. These motions have been studied by such techniques as NMR, dielectric relaxation, ultrasonic attenuation, dynamical light scattering, fluorescence depolarization, and excimer fluorescence. However, these experiments do not reveal many of the details about the motion, such as whether correlations exist between transitions of near neighbors, or, in general, what the effect of the rest of the chain is on the bond undergoing the transition. That the rest of the chain, what we term the tails, plays some role is evident. Clearly, as a particular bond rotates, the attached tails cannot rigidly follow without experiencing a huge frictional resistance.

What experiment does reveal is that there are relaxation processes taking place, and, for example, in substituted polystyrenes in solution, they are on a time scale of 0.1–10 ns.[1] The rates are inversely proportional to solvent viscosity, indicating that the dynamics may be regarded as high-friction Brownian motion. Activation energies vary a bit with the technique but are about 20 kJ. Of this perhaps 10 kJ should be attributed to the temperature dependence of the solvent viscosity. The 10 kJ which remains is an energy comparable to the barrier height between the trans and gauche states. Indeed, Liao, Okamoto, and Morawetz[2] find the temperature dependence of excimer fluorescence intensity in a polymer parallels that in a small molecule analogue. In fairness, one should mention the sound absorption experiments of Cochran, Dunbar, North, and Pethrick[3] which imply a contradictory conclusion; viz., the activation energy in a polymer system is more than twice as large as that in small or intermediate size molecules.

The question of whether the activation energy is one or two barrier heights is central because of a proposal which has been advanced regarding how conformational transitions can occur without experiencing much resistance from the tails. There are certain modes of motion (generally called crankshafts), such as the Schatzki crankshaft[4] or the three-bond motion,[5] which leave the tails in the same position at the start and end of the transition. Such motions involve two barrier crossings, or the passage through some fairly high energy intermediate state. This is the motivation for the careful examination of activation energies in various experimental works and in the present report. Like most of the experimentalists, we find an activation energy close to one barrier height.

Actually, there is no reason why one should turn to motions such as crankshafts, especially three-bond motions, to explain conformational transitions in polymers. As has been explained by Keck[6] and Bennett,[7] one may calculate transition rates from an initial equilibrium distribution of states centered around the bottleneck (reaction barrier). Therefore the state of the tail in the energy *well* of the original conformation is of little pertinence, nor, for that matter, is the state of the tail in the final, minimum-energy state. What is important is the nature of the motion as one traverses the reaction barrier. One must study the nature of the reaction coordinate (path of steepest descent) and trajectories which fluctuate about it. This is recognized in the theory of Skolnick and Helfand,[8] which will be compared with the Brownian simulation results in section V. Cooperative transitions may occur, though. One transition may induce another in a kind of counter-twist mode. For these reasons it is of interest to examine the degree and nature of cooperative pairs of transitions which show up in the simulations.

There have been a number of other computer simulation studies of conformational transitions in chain systems. A one-dimensional chain of bistable oscillators is a model which shares many of the important features of the isomerization kinetics of carbon backbones. This model has been simulated by Weiner and Pear[9] and by Helfand.[10] In the latter case the transition kinetics have been analyzed in a manner similar to that employed here. Brownian dynamics has been performed on moderate sized chains with rigid bonds and angles by Fixman,[11] Pear and Weiner,[12] Levy et al.,[13a] and Evans and Knauss.[13b] An impulsive, stochastic-dynamics study has recently been reported by Chandler.[14] Molecular dynamics has been performed on short-chain systems by Ryckaert and Bellemans[15] and Weber[16] while polymers have been simulated by Weber and Helfand.[17]

The study reported on in this paper has been briefly summarized earlier.[18] We call attention to the fact that the table of reaction rates in that paper is to be replaced by Tables II–V of this paper, which represent better data analysis. The new rates also imply a slightly higher activation energy (see section III).

The plan of the present paper is as follows. In section I the polymer model is described, and the solution of the Langevin equations, which govern the motion, is outlined. The question of how to go from representative trajectories to transition rates is addressed in section II and illustrated with an analysis of the conformational transition rate in butane. In sections III–V results of the simulations of macromolecules are analyzed to extract transition rates and activation energies. The data are examined particularly with an eye toward gleaning information about cooperativity of transitions. The results are compared with a recent theoretical calculation and explanations are advanced for some of the most striking observations. The paper is ended with a summary of the major conclusions.

I. Molecular Model and Simulation Scheme

The motions to be simulated are governed by a backbone potential affecting bond lengths, bond angles, and torsional

‡ This paper is dedicated, with great pleasure and appreciation, to Professor Paul J. Flory on the occasion of his 70th birthday.

0024-9297/80/2213-0526$01.00/0

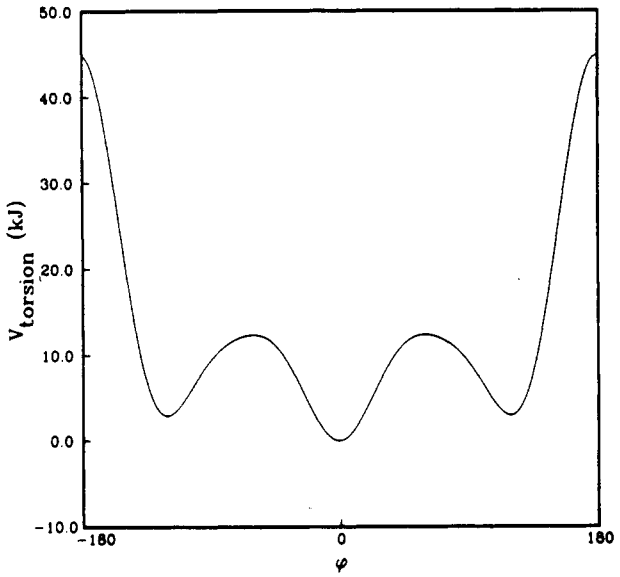

Figure 1. Potential for bond rotation as a function of torsional angle. Trans corresponds to $\phi = 0$.

angles. The bond lengths, b_i (distance from vertex $i-1$ to i), are kept close to a value b_0 by a potential

$$v_b(b_i) = \tfrac{1}{2}\gamma_b(b_i - b_0)^2 \qquad \text{(I.1)}$$

with γ_b the bond-stretching force constant. The bond angles, θ_i (angle at vertex i between bond vectors $i-1$ and i, e.g., 70.53° for tetrahedral bonding), are kept near θ_0 by a potential

$$v_\theta(\theta_i) = \tfrac{1}{2}\gamma_\theta(\cos\theta_i - \cos\theta_0)^2 \qquad \text{(I.2)}$$

Bond rotation, specified by the torsional angles ϕ_i (zero for trans), takes place in a rotational potential, as depicted in Figure 1, of

$$v_\phi(\phi_i) = \gamma_\phi \sum_{n=0}^{5} a_n \cos^n \phi_i \qquad \text{(I.3)}$$

with $a_0 \equiv 1$, and

$$\sum_{n=0}^{5} a_n = 0 \qquad \text{(I.4)}$$

The latter condition sets the zero of energy as trans. There are actually five independent constants in this potential, which may be specified as: the height of the trans-gauche barrier, E^*; the energy difference between the trans and gauche minima, E_g; the energy at the cis state, E_{cis}; the angular location of the barrier, ϕ^*; and the angular location of the gauche minimum, ϕ_g.

Simulations were performed with two different choices of the potential parameters, as listed in Table I. The torsional potential for the A set is as proposed by Ryckaert and Bellemans.[15] The B set, used in some initial work, involves a cubic, rather than quintic, in eq I.3. More detailed analysis has been done with the A-set simulations, and all discussions in this paper will relate to this potential unless there is an explicit statement to the contrary.

Several additional remarks should be made about the potential.

1. The parameters γ_t, γ^*, and γ_g in Table I are the magnitudes of the curvature of the torsional potential, v_ϕ, at the trans minimum, the trans-gauche barrier, and the gauche well, respectively; i.e.,

$$v_\phi = \tfrac{1}{2}\gamma_t\phi^2 \qquad \text{near trans}$$

$$v_\phi = E^* - \tfrac{1}{2}\gamma^*(\phi - \phi^*)^2 \qquad \text{near the barrier}$$

$$v_\phi = E_g + \tfrac{1}{2}\gamma_g(\phi - \phi_g)^2 \qquad \text{near gauche}$$

Table I
Parameters of the System

property	potential A	potential B	units
$\beta = \zeta/m$	1.0×10^5	1.0×10^5	ns^{-1}
m	0.014	0.014	kg/mol
b_0	0.153	0.154	nm
γ_b/m	2.5×10^9	2.5×10^8	ns^{-2}
θ_0	70.53	66.70	deg
γ_θ/m	1.3×10^7	1.5×10^7	J/kg
γ_ϕ/m	6.634×10^5	2.539×10^5	J/kg
a_0	1	1	
a_1	1.3108	3.3949	
a_2	-1.4135	4.9086	
a_3	-0.3358	-9.3035	
a_4	2.8271	0	
a_5	-3.3885	0	
E^*	12.36	9.977	kJ/mol
E_g	2.933	2.095	kJ/mol
E_{cis}	44.833	42.0	kJ/mol
ϕ^*	±60	±55.5	deg
ϕ_g	±120	±102.4	deg
γ_t/m	5.412×10^6	3.732×10^6	J/kg
γ^*/m	1.903×10^6	3.759×10^6	J/kg
γ_g/m	7.530×10^6	5.281×10^6	J/kg

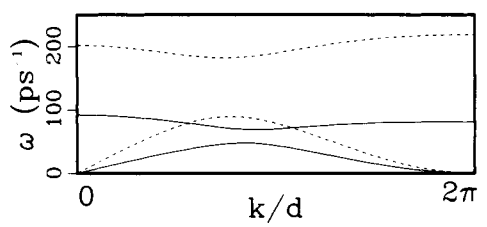

Figure 2. Spectrum for in-plane vibrations of an all-trans chain linear hydrocarbon. The dashed lines correspond to the experimental force constants.[19] These motions have been slowed by adoption of the γ_b and γ_θ of Table I, which leads to the spectrum shown by the solid curve. The wave vector k is scaled by the repeat length d separating alternate carbons.

2. The parameters of the torsional potential are selected as representative of a hydrocarbon chain. However, the force constants for the bond stretching and angle bending have been somewhat decreased. The purpose is to slow down these fastest oscillations which control how small the time step for numerical integration must be. A more realistic estimate for γ_b and γ_θ might have been $\gamma_b/m = 1.8 \times 10^{10}$ ns^{-2} and $\gamma_\theta/m = 4.2 \times 10^7$ J/kg.[19] Such values would lead to a vibrational spectrum for the in-plane motions of an all-trans chain as shown by the dashed line in Figure 2. The solid line corresponds to the force constants we have adopted. The smaller force constants produce a slowing of the bond stretching and angle bending oscillations, but also make it easier to distort these modes. Even though these modes are only slightly distortable altogether, we expect that the reaction coordinate is affected. Specifically, it is easier to create localized modes (discussed in section V), so the transition rate is slightly increased. However, it is to be expected that qualitative features of the transition are not seriously disturbed.

3. A number of authors[11-13,15] have chosen to study the conformational dynamics of chain molecules, using a model in which bond lengths and angles are fixed. The considerable differences between such rigid constraints and flexible constraints, even with high force constants, have been discussed elsewhere.[20] In addition, rigid constraints should severely modify the nature of the reaction coordinate.

4. No explicit interactions between the carbon centers along the chain have been included. Therefore the macromolecule is what is frequently called a phantom chain, one that can pass through itself. Also the equilibrium

conformation does not have the "pentane effect" (near exculsion of $g^{\pm}g^{\mp}$ pairs) and excluded volume characteristics. Hydrodynamic interactions between carbon centers, transmitted by the surrounding medium, have also not been included. The rapid conformational transition processes studied here should not be seriously affected by the omission of these terms.

5. While it is theoretically possible for a bond angle to pass through 0°, which would look like a sudden 180° rotation, this is unlikely since $v_\theta(0) = 81$ kJ. The probability of a bond passing through zero length is even lower since $v_b(0) = 819$ kJ.

The simulations have been performed on a system of 200 carbon centers. In order to avoid end effects, and make every bond statistically equivalent, the chain is closed into a ring by putting a bond between the 200th and the first vertex. (The alternative procedure[17] of periodically repeating an open chain to make it into an infinite polymer is yet to be tried in these Brownian simulations.) We believe that the closure into a ring has only a minor effect on the short-time dynamics. In addition to the macromolecule studies, conformational transitions have been looked at in open *n*-butane and *n*-octane chains, but will only be discussed peripherally here.

The equations which describe high-friction Brownian motion are the Langevin equations in which the inertial term is set to zero, i.e., is regarded as minor relative to the forces. Thus, the force of frictional resistance is taken as being equal in magnitude and opposite in direction to the sum of the potential force and the Brownian random force. This yields the equation of motion (it is convenient to divide by the mass of the particle):

$$\beta \, d\mathbf{r}_i/dt = -(1/m)\nabla_{\mathbf{r}_i} V + \mathbf{A}_i(t) \qquad (I.5)$$

Here β, with units of reciprocal time, is the friction constant ζ divided by the particle mass m (ζ and m are taken as the same for all particles in the present work). V is the total potential, a sum of the v_b's, v_θ's, and v_ϕ's. The random force (per unit mass), $\mathbf{A}_i(t)$, is Gaussianly distributed with mean zero and covariance

$$\langle \mathbf{A}_i(t)\mathbf{A}_j(t')\rangle = (2\beta k_B T/m)1\delta_{ij}\delta(t - t') \qquad (I.6)$$

where $k_B T$ is Boltzmann's constant times the temperature. According to experiments, the high friction limit seems appropriate for the description of conformational transitions. This limit does not properly describe the bond length and bond angle vibrations, but the conformational transition processes should not be overly sensitive to the detailed trajectories of these fast motions. All that is required is a process which rapidly produces a proper distribution of bond angles and lengths in the field generated by the slower torsional motions.

For the present work we have chosen $\beta = 10^{-5}$ ns^{-1} as a representative value. Note, however, that the value of β only sets the absolute time scale since β and t enter the equation of motion, eq I.5 and I.6, only in the combination t/β. The transition rates we find are proportional to $1/\beta$, and can easily be converted to any other β the reader considers appropriate.

Generating a numerical solution to an equation of motion means determination of a sequence of points along the trajectory at time intervals s: $\mathbf{r}_i(0)$, $\mathbf{r}_i(s)$, $\mathbf{r}_i(2s)$, ... We used time steps of $s = 5 \times 10^{-6}$ ns. Of course, there is no definite trajectory for stochastic differential equations such as eq I.5. A numerical procedure attempts to select positions $\mathbf{r}_i(s)$, given $\mathbf{r}_i(0)$, as if they had been drawn from a statistical population dictated by the transition probability corresponding to the stochastic differential equation. For this purpose we have used the recently proposed[21] stochastic extension of the Runge-Kutta method and gone to second order. The technique is an improvement over that employed in the linear chain simulations.[10] Some quantitative measures of its efficacy are discussed in the Appendix.

All simulations were carried out until over 4000 transitions had occurred. A nanosecond of simulation of the 200-bond chain took 35 h on a Harris/7 computer.

II. Analysis of the Trajectory for Transition Properties

When looking at the trajectory generated in a simulation, one sees diffusive motion about the local minimum energy states corresponding to the rotational isomeric states, with occasional transitions to another well. In order to extract from this trajectory information about the transitional kinetics we have used an analysis of first passage times, similar to that of ref 10. The technique is best explained in the context of butane simulations, where there is only one torsional angle, ϕ, to follow.

Associated with the simulation is a clock. We know in which region of the v_ϕ diagram the angle ϕ is (gauche-plus, trans, or gauche-minus). When ϕ arrives at the minimum of one of the other wells we record the time and reset the clock to zero. Thus we get a set of times which represent the first passage times form one minimum well angle to another. It is somewhat arbitrary that we require the torsional angle to go over an energy maximum and all the way to the next minimum before regarding the transition as complete. Certainly, one does not want to count as a transition every passage over the barrier, since in the diffusion process the angle moves back and forth over the barrier many times during a passage.

The information contained in the set of first passage times is best depicted in a hazard plot. The hazard rate $h(t)$ is defined such that $h(t)\,dt$ is the probability that a bond, which has not had a transition in a time t since the last transition, has a transition between t and $t + dt$. It is more convenient to prepare a plot which displays the (cumulative) hazard

$$H(t) = \int_0^t h(t')\,dt' \qquad (II.1)$$

and to examine the slope as a measure of transition rate. The probability, $P(t)$, that a bond has the next transition in a time less than t since the last transition is related to the hazard by

$$P(t) = 1 - \exp[-H(t)] \qquad (II.2)$$

The details of how to prepare a hazard plot from the first passage times are given in ref 10.

In Figure 3 we see a hazard plot for a butane stochastic dynamics simulation at $T = 425$ K. The plot is nearly a straight line with a slope of $\lambda = 67.1$ ns^{-1}. The rate thus measured is a composite of all processes, trans going to either one of the gauches or vice versa:

$$\lambda = 2p_t\lambda_{tg} + 2\,p_g\lambda_{gt} \qquad (II.3)$$

where λ_{tg} is the rate of transition from trans to one of the gauches, λ_{gt} is the reverse rate, p_t is the fraction of trans, and p_g is the fraction in *one* of the gauche states. Detailed balance requires that

$$p_t\lambda_{tg} = p_g\lambda_{gt} \qquad (II.4)$$

so that

$$\lambda_{tg} = \lambda/(4p_t) \qquad (II.5)$$

which is 29.6 ns^{-1} for this butane simulation.

Actually, the rate λ was not determined visually from the graph, or even by a least-squares fit. Rather, this was

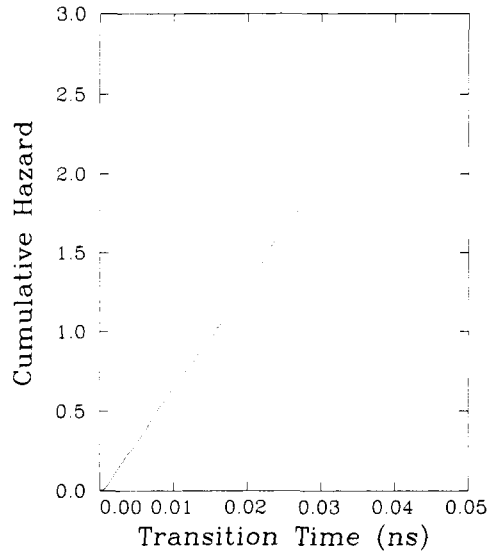

Figure 3. Hazard plot for the 425 K Brownian dynamics simulation of butane. The slope is the rotational transition rate.

Table II
Transition Rates for Two Potentials and Various Temperatures[a]

T, K	E^*/k_BT	λ_{tg}, ns^{-1}	f_{tg}	c_0, %	p_t
		Potential A			
425	3.5	7.0	232	37	0.569
372	4.0	4.0	217	37	0.597
330	4.5	2.2	202	35	0.626
297	5.0	1.2	173	48	0.653
		Potential B			
400	3.0	16.8	317	31	0.533
300	4.0	5.8	315	34	0.582
240	5.0	1.9	284	37	0.631

[a] Hazard fit to eq III.3 by least squares, excluding the short time region.

done by a maximum likelihood estimation of the parameters of a functional fit to the hazard[10,22] (this is a technical point not required for physical understanding).

There are other approaches to the analysis of reaction rates which we are also investigating. Correlation functions are conventional, but it is more difficult to extract fundamental information from them. Nevertheless, they should be examined because of their close connection to measurement processes. The method of reactive flux[6,7,14] is appealing, and will be applied by us in the near future.

III. Polymer Conformational Transition Rates

As mentioned, the model studied is a ring of 200 bonds with a realistic backbone potential creating typical polymeric geometry. Because the bonds are identical, the first passage times for the transitions of all the bonds can be combined. The solid line of Figure 4 shows a hazard plot prepared from the data on a 372 K run, $E^*/k_BT = 4.0$. The transition rate, λ, is the asymptotic slope.

The λ's for the various temperature runs of potentials A and B have been determined and transformed to λ_{tg}'s according to eq 2.5, with p_t calculated by integrating the Boltzmann factor $\exp[-v_\phi(\phi)/k_BT]$ from $-\phi^*$ to $+\phi^*$ and normalizing. The results are reported in Tables II and III (representing two fitting procedures described later). The rates λ_{tg} are given directly and also in the form of a prefactor f_{tg} defined by

$$\lambda_{tg} = f_{tg} \exp(-E^*/k_BT) \qquad \text{(III.1)}$$

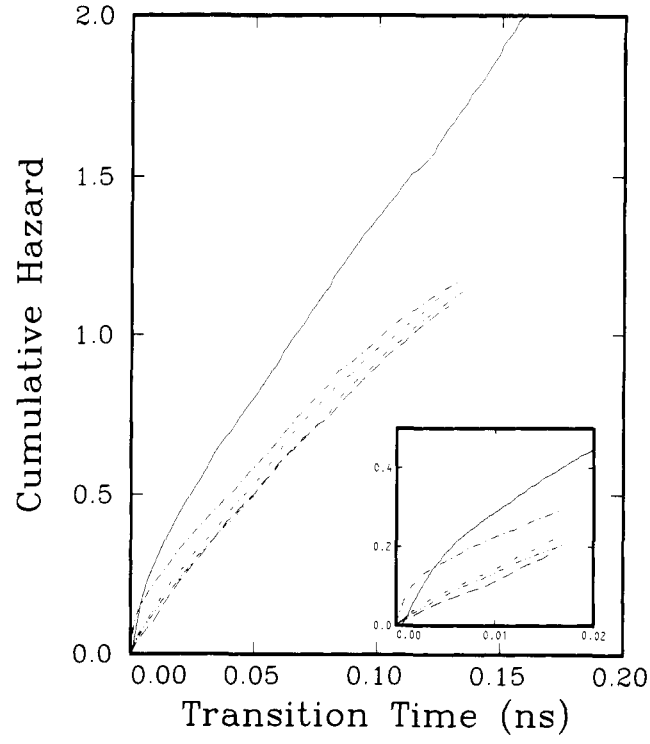

Figure 4. Hazard plot for the 372 K simulation of the polymer chain. The solid curve relates to the times from one rotational transition of a bond to the next of that bond. Other curves are transitions of neighbors measured from the time of last transition of the central bond (m = 1, dashed; m = 2, dot-dashed; m = 3, dot-dot-dashed; m = 4, dot-dot-dot-dashed). The short time region, magnified at the lower right, shows the enhanced transition rate (greater slope) for back transitions of the same bond, and for correlated transitions of neighbors.

Table III
Transition Rate[a]

T, K	E^*/k_BT	λ_{tg}, ns^{-1}	f_{tg}	c_0, %
		Potential A		
425	3.5	7.7	256	25
372	4.0	4.6	249	21
330	4.5	2.5	222	22
297	5.0	1.5	216	22
		Potential B		
400	3.0	16.3	327	27
300	4.0	6.3	343	23
240	5.0	2.2	323	21

[a] Hazard fit to eq III.7 by the maximum likelihood estimation.

An Arrhenius plot of the rates from Table III, Figure 5, gives an activation energy of $E^\ddagger = (1.12 \pm 0.02)E^*$ for potential A and $E^\ddagger = (1.01 \pm 0.03)E^*$ for potential B. The uncertainties are a standard deviation in the least-squares fit of the Arrhenius plots and do not reflect the even greater uncertainty involved in extracting λ from the data. The activation energies are slightly greater than one barrier height. The hypothesis that $E^\ddagger$ is one barrier height is probably tenable but the hypothesis that it is $2E^*$ is probably not.

Unlike the butane simulation, the hazard plot in Figure 4 is not a straight line in the short time region. Rather, the slope is higher, indicating a higher rate of transition. Since small t means short times since the last transition, one sees that immediately after one transition occurs there is an enhanced rate for another transition. If the first transition was $t \rightarrow g^\pm$ (trans goes to gauche plus or minus), then the second is almost always the reverse, since the cis

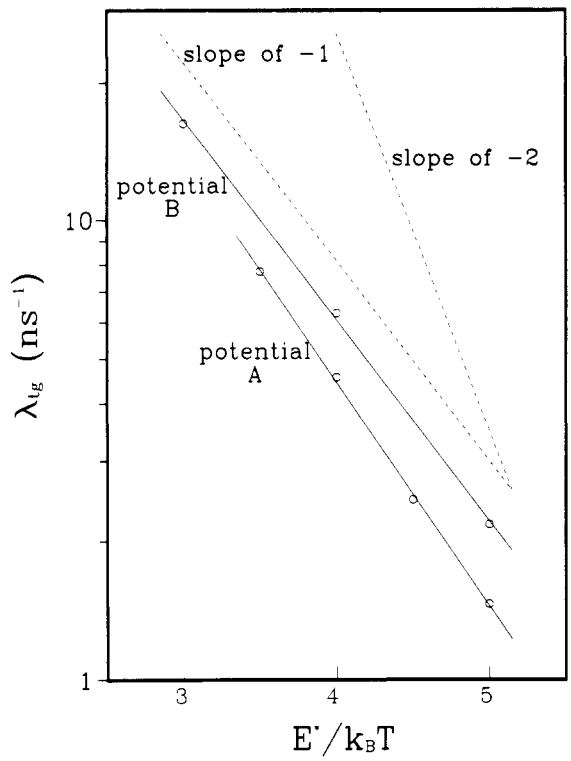

Figure 5. Arrhenius plot of the logarithm of the transition rate vs. E^*/k_BT.

barrier is quite high (we have rarely observed a cis barrier crossing). However, $g^{\pm} \rightarrow t$ can be followed by either the reverse or by $t \rightarrow g^{\mp}$. Consider all the pairs of transitions of the same bond which occur in a time interval where there is significant curvature in the hazard plot (e.g., $<5 \times 10^{-3}$ ns for 372 K). Of the 203 pairs for which the first state is gauche, 184 go back to this gauche, while 19 go to the other gauche. The major reason for the enhanced short time transition rate thus appears to be that when a transition occurs the neighbors may not be in, or relax into, a position which can accept this new conformation. Therefore the bond is forced back to the original state. This shows that it was not completely sufficient to take the movement of the torsional angle all the way to the bottom of a new well as a criterion for the completion of a transition.

One also notes in Figure 4, especially in the short time blowup, that the hazard curve does not come in to zero at zero time. This is merely a reflection of the finite time required to get from one energy minimum to another, even if there was no barrier. By extrapolation from higher times one can arrive at a time, t_0, which should be subtracted from the first passage times of the bond angle before analysis is begun. In all that follows this has been done, and first passage times less than t_0 have been set to t_0. References to $t = 0$ really mean $t = t_0$. (This is a minor correction.)

There are various analytical approximations which one can use to describe the hazard curve. Consider, first, that all the uncompleted reactions which reverse are regarded as reversing instantly and that thereafter the transitions to new states are a Poisson process with rate λ_0. In that case the rate of transition (hazard rate) is

$$h(t) = \lambda_0 + \nu_0\delta(t-) \qquad \text{(III.2)}$$

where the physical meaning of ν_0 will emerge below. The cumulative hazard (integral of h, eq II.1) is

$$H(t) = \lambda_0 t + \nu_0 \qquad \text{(III.3)}$$

According to eq II.2, the probability of a transition having occurred in a time less than t is (this equation is given incorrectly in eq 3.1 of ref 10)

$$P(t) = 1 - (1 - c_0)\exp(-\lambda_0 t) \qquad t > 0 \qquad \text{(III.4)}$$

$$c_0 = 1 - \exp(-\nu_0) \qquad \text{(III.5)}$$

From the fact that $P(0+) = c_0$ we can identify c_0 as the fraction of "transitions" (according to the well-to-well criterion) that immediately reverse. A measure of c_0 can be obtained by fitting the asymptotic portion of the hazard plot with a straight line and using the intercept, ν_0, in eq III.5. The fit has been done by least squares, omitting the data in the short time, severely nonlinear region. (A maximum likelihood estimate with censoring,[10,22] used in ref 18, has some statistical inconsistencies.)

A better functional fit to the transition rate spreads the consecutive processes over some time span σ_0 with an exponential law

$$h(t) = \lambda_0 + (\nu_0/\sigma_0)\exp(-t/\sigma_0) \qquad \text{(III.6)}$$

$$H(t) = \lambda_0 t + \nu_0[1 - \exp(-t/\sigma_0)] \qquad \text{(III.7)}$$

In this fit ν_0 may again be used to calculate a fraction of "transitions" which reverse before stabilizing, using eq III.5. To achieve a fit with eq III.7, maximum likelihood estimation techniques are best.

In Table II are the transition rates for the various simulations, determined as a fit to the linear hazard, eq III.3. Also presented are the c_0's, the fraction of transitions which immediately follow an earlier transition. In Table III are the rates and c_0 according to a fit to the three-parameter eq III.7. The differences between the two tables are some measure of the considerable uncertainty inherent in the data fitting.

The argument might be made that the rates reported are actually too high because of the fraction, c_0, of transitions which almost immediately reverse themselves. A barrier crossing should not have been counted as a transition unless the barrier is crossed an odd number of times. The probability of an odd number of crossings is[16] $1/(1 + c_0)$, so that a better estimate of the rate of true transitions is $1/(1 + c_0)$ times the rates in the tables. We have not made these corrections because of the great uncertainty in c_0 and because of the general ambiguity in defining transition rates of processes defined on a continuum.

IV. Correlation of Transitions

The closeness of the activation energy to one barrier height is some indication that conformational transitions in chain molecules do not have to occur as cooperatively as is implied by crankshaft theories. The fairly good agreement of the simulated rates with calculations which neglect cooperative transitions (section V) lends further credence to this point of view. Nevertheless, a direct examination of the problem reveals a picture that is somewhat more complex.

In order to investigate the question of cooperativity between transitions of neighboring bonds we returned to a study of first passage times. It has already been noted that in the computer a "clock" was associated with each bond, and that the clock was set to zero whenever a transition occurred (first appearance at a new potential well). Now, instead of measuring the next transition time for that bond (hereafter called the central bond), we recorded the first passage time of the mth neighbor, with $m = 1$–4 and in a few cases $m = 6$. Hazard plots (Figure 4) of these transition times have slopes which are the rate of transition of the bond at a time measured from the last

Table IV
Characteristics of mth Neighbor Transitions[a]

T, K	c_1, %	c_2, %	c_3, %	c_4, %	λ_{1tg}, ns^{-1}	λ_{2tg}, ns^{-1}	λ_{3tg}, ns^{-1}	λ_{4tg}, ns^{-1}
				Potential A				
425	10	18	8	10	5.6	5.5	6.1	5.9
372	12	21	10	14	2.8	2.8	3.1	2.9
330	9	20	10	11	1.7	1.7	1.7	1.8
297	10	22	11	15	0.82	0.82	0.86	0.82
				Potential B				
400	13	17	12	10	11.7	12.6	12.4	12.9
300	9	18	11	12	4.3	4.4	4.3	4.6
240	9	18	9	10	1.4	1.4	1.5	1.5

[a] Fit to eq III.3 by least squares over the linear range.

Table V
Characteristics of Second Neighbor Transitions[a]

T, K	c_2, %	σ_2, ps	λ_{2tg}, ns^{-1}
	Potential A		
425	12	1.1	6.5
372	12	1.5	3.4
330	12	1.9	1.9
297	12	2.5	1.1
	Potential B		
400	12	0.73	14.1
300	12	1.4	5.0
240	10	1.9	1.7

[a] Fit to eq III.7 by the maximum likelihood estimation.

transition of the central bond. In Figure 4 concentrate particularly on the short time region, shown magnified. A striking observation is the greatly enhanced rate of transition of the second neighbors (slope), lasting for a short time. These data have been fit to eq III.3 and III.7 with results shown in Tables IV and V, respectively. One sees from the values of c_2 that in all cases some 10–20% of the transitions of second neighbors can be regarded as following transitions two bonds away in a correlated fashion. When one considers that c_2 reflects only the second of two transitions involved in the correlated process, one realizes that a significant number of the conformational transitions must be regarded as being involved in a correlated process.

The hazard plots for neighbors other than the second are qualitatively different, as one can see in Figure 4. They do not show a large increase in rate for a short period of time. They do show slight curvature spread over a longer period of time. This may be an indication of some type of correlation. However, even when we look at the 25th and 50th neighbor, curvature in the hazard plots is observed. Part of this can be attributed to the non-Poisson nature of the individual bond's transition process. An effort to understand this longer term curvature is underway. In order to provide some measure of the correlation which might be reflected in the data, we have included in Table IV values of c_1, c_3, and c_4 based on a linear, least-squares fit to the data with exclusion of a short time region. This analysis is to be regarded as extremely tentative.

V. Theory and Interpretation

Recently Skolnick and Helfand[8] have developed a reaction rate theory for the determination of conformational transition rates in molecular systems and applied it to the model employed in the present simulations. There are several aspects to a reaction rate theory. One assumes that states are defined as regions of the multidimensional configuration space of all the atoms. The surfaces dividing regions usually pass through energy saddle points and continue along the paths of most rapid ascent up the mountains of energy. The rate of transition from state A to state B is given as the average rate of passage from region A to B of members of a statistical ensemble, with the proviso (not uniquely defined) that the system equilibrate in the B state before passing on to another state or back to A. In transition state theory the rate of passage across the dividing surface is given by the equilibrium probability density of being at the divide times the equilibrium mean outward velocity across the barrier. There are several reasons for a return across the barrier before equilibrium is achieved. One is interaction with the medium, which here and in ref 8 is treated as a Brownian random force in the high friction limit (high friction limit is an approximation easily removed). The second reason for return is anharmonicity of the potential (which is sometimes cast into the form of an internal friction). A special type of anharmonicity is the possibility of transitions of neighboring bonds. The theory of ref 8 treats the passage over the barrier in harmonic approximation about the saddle point. Therefore there is no provision for neighbor transitions, nor for any internally induced back-reaction. The medium effects are accounted for by determining the diffusion current across the barrier rather than the mean velocity. (This is the difference between Kramers' theory[23] and the transition state theory.) In the harmonic approximation the key step is the determination of the reaction coordinate, which is the path of steepest descent from the saddle point. One finds that the reaction coordinate in the present case is a localized mode. It involves torsional rotation of the central, transforming bond and distortions of the neighboring degrees of freedom which fall off with distance from the transition center. The distortions must occur so that remote units of the tails attached to the transforming bond do not have to move. The nature of the localized mode depends on the conformation of the neighbors of the transforming bond. The easiest degrees of freedom to distort are other torsion angles. When the first neighbor of a central, transforming bond is trans then the second neighbor bond is parallel to the central bond. When the central bond undergoes rotation, a counter rotation of the second neighbor is an important component of the reaction coordinate, and the reaction coordinate remains rather localized. On the other hand, with other conformations of the neighboring bonds torsional angle distortion cannot be as effectively utilized to take up the central bond's motion, and the localized mode spreads further down the tail. The more units that move in the reaction mode, the higher the frictional resistance, and the slower the transition rate.

Using this theory, and performing a thermal average over conformations of the tails, one predicts[8] the transition rate for a bond of the simulated polymer with potential A to be 1.86 ns^{-1} at T = 372 K, compared to the simulated value of 4.6 ns^{-1}. Sources of the discrepancy are the failure to correct the simulation for back reaction, uncertainty in analysis of data, and neglect of anharmonicity. As a gauge of the effectiveness of the theory in less complicated cases it should be noted that the theory predicts a transition rate, λ_{tg}, for butane at 425 K of 30.0 ns^{-1}, compared to a simulated value of 29.5 ns^{-1}. The predicted rates for the three types of bonds of octane (from outer toward central) are 18.6, 13.7, and 9.8 ns^{-1}, compared with simulated values of 20.3, 14.3, and 13.0 ns^{-1}.

The degree to which trans first neighbors of a transforming bond allow for a more rapid reaction can be seen clearly by examining a list of the simulated transitions. In Table VI we have categorized the transitions which occurred during the various potential A simulations. The

Table VI
Evidence for First Neighbor Trans Enhancement of the Transition Rate

temp, K	state j[a]	n_j[b]	$n_j/n_{tot}p_j$[b]
425	*tst*	1800	1.39
	tsg or *gst*	1955	1.00
	gsg	245	0.33
372	*tst*	1700	1.23
	tsg or *gst*	1955	1.01
	gsg	299	0.46
330	*tst*	2099	1.34
	tsg or *gst*	1698	0.90
	gsg	216	0.38
297	*tst*	2307	1.34
	tsg or *gst*	1572	0.86
	gsg	148	0.31

[a] The central bond s undergoes some transition. The states j are the possible conformations of the first neighbors. [b] The number of transitions with neighbors in state j, n_j, is divided by the total number of transitions at that temperature, n_{tot}, and divided by the probability of state j, p_j.

state of the two first neighbors of the transforming bond is indicated, together with the number of transitions of the bond centered between these states. To reduce the data to comparable terms we have divided the number of transitions of each type by the total, to produce fractions. Then we divided each fraction by the probability of occurrence of the pair of neighbor states. One sees that the rate of transition is three or four times faster when both neighbors are trans as opposed to both gauche. With only one trans neighbor the reaction coordinate motion has been theoretically shown[8] to shift over to the trans side, and the rate is only slightly down from that of two trans neighbors, as predicted.

The effect of a trans first neighbor is even more striking in relation to the cooperative pairs of transitions analyzed in the previous section. We again recall that whenever there is a trans bond in a polymer then the two adjacent bonds, second neighbors to each other, are parallel. For a motion in which the bond on one side of the trans rotates $+\phi$ and the bond on the other side rotates $-\phi$, the tails translate rather than rotate, as was pointed out in ref 24. This may manifest itself as a pair of transitions of second neighbors, such as in gauche pair production or annihilation

$$ttt \rightleftarrows g^{\pm}tg^{\mp}$$

or gauche migration

$$g^{\pm}tt \rightleftarrows ttg^{\pm}$$

To observe whether these motions show up significantly in the simulations we again looked at a short time period, τ (0.005 ns for the conditions of Figure 4), in which the cooperative, second-neighbor pair transitions mostly occur. In Table VII are listed all such transitions and the number of times they occur in τ. (Although only the results for the 372 K simulation are displayed, the other simulations reveal the same pattern of observations.) Consider, for example, the production of a gauche pair

$$tst \rightleftarrows g^{\pm}sg^{\mp}$$

where s represents the conformational state of the intermediate bond. When s is trans, 407 such transitions occur in time τ, whereas when s is gauche there are only 25 such transactions. Likewise for gauche migration,

$$g^{\pm}st \rightleftarrows tsg^{\pm}$$

Table VII
Numbers of Each Type of Pair Transition in the Initial 0.005 ns of the 372 K Simulation

transition[a]	no. of occurences	transition[a]	no. of occurrences
$\pm tt \rightleftharpoons tt\pm$	523	$\pm\pm t \rightleftharpoons t\pm\pm$	8
		$\mp\pm t \rightleftharpoons t\pm\mp$	25
$\pm tt \rightleftharpoons tt\mp$	27	$\pm\pm t \rightleftharpoons \pm\mp t\pm\pm$	50
$ttt \rightleftharpoons \pm t\mp$	407	$t\pm t \rightleftharpoons \pm\pm\mp t\pm t \rightleftharpoons \mp\pm\pm$	25
$ttt \rightleftharpoons \pm t\pm$	32	$t\pm t \rightleftharpoons \pm\pm\pm$	53
		$t\pm t \rightleftharpoons \mp\pm\mp$	7

[a] $\pm$ and $\mp$ represent $g^{\pm}$ and $g^{\mp}$, respectively.

one finds 523 transition pairs when the central bond is trans and only 33 when it is gauche. (These striking effects are certainly not due to the ratio of the probabilities of s being trans to gauche, which is only 1.48.)

Some attention should be paid to the fact that there are 60 transitions of the type $tgt \rightleftarrows g^{\pm}gg^{\pm}$ but only 25 of the type $tgt \rightleftarrows g^{\pm}gg^{\mp}$. Note that the two bonds surrounding the central gauche have an angle between their bond vectors of 109.5°, which is more antiparallel than parallel. That may explain why there is a preference for rotations of these bonds in the same direction, rather than counter. The same effect shows up in gauche migration.

VI. Conclusions and Interpretation

Brownian dynamics simulations are a useful means of probing the kinetics of conformational transitions in polymers to develop both a quantitative and a qualitative picture. Several of the conclusions drawn in a recent theoretical study seem to be borne out. The rates can be reasonably approximated by concentrating on the region of the configuration space in the neighborhood of the reaction barrier. (This plays down the role of crankshaft motions.) Importance is attached to creating a localized mode as a reaction coordinate. The presence of trans first neighbors to a transforming bond implies second neighbor bonds parallel to the central, transforming bond. These appear to be useful in taking up the rotational motion of the central bond and localizing the mode. In fact, the counter rotation of the second neighbors frequently shows up as a cooperative transition.

It is our feeling that additional analysis of simulations will be valuable in developing a picture of the fundamental features of conformational transition kinetics. More theoretical guidance would be useful to indicate how the fine features of the transition process can be effectively probed.

Appendix. Measure of the Efficacy of the Numerical Stochastic Differential Equation Integrator

When one integrates a deterministic differential equation, a measure of efficacy of the integrator is how accurate the trajectory is. This is usually studied by halving the time step or from error estimation formulas. For molecular dynamics simulations (nonstochastic) such a technique is not practical, and attention usually focuses on the extent to which constants of the motion, such as energy, are conserved. A stochastic equation of motion neither has a definite solution nor conserves energy. Only statistical properties need be correct for long time averages. One measure of the statistical properties is the temperature. Since there are no velocity variables in the high friction limit, the temperature cannot be measured as a mean kinetic energy. However, temperature is a variable in the configurational distribution function, which provides a

route to its measurement. Because of the additive nature of the potential energy, the distribution function of a chain is factorable into a product of bond length distributions, bond angle distributions, and torsional angle distributions. Each is proportional to $\exp(-v/k_BT)$ with the appropriate v. Closing the chain into a ring actually ruins this factorizability, but the effect is small for a large ring, and will be ignored. Let there be given a set of observed values of a stochastic variable, x, which is distributed according to a probability density $f(x,T)$, with T a parameter. An estimate of T can be obtained by maximum likelihood estimation[22] (which is better than a moment technique). In this way a temperature for the bond length and bond angle distributions was determined. After short initial aging the estimate is quite stable. As an example, consider the simulation for potential A at a temperature 330.4 K, imposed by the strength of the random force according to eq I.6. Over 512 550 time steps of 5×10^{-6} ns, the temperature of the bond lengths is found to be 323.0 K and that of the bond angles 329.4 K. As expected, the result for the bond lengths is the worse because the ratio of the time step to the shortest vibration time is greatest. The temperature for the torsion angles was not determined, but it should be very good because these are the slowest modes.

References and Notes

(1) K. Matsuo, K. F. Kuhlmann, H. W.-H. Yang, F. Gëny, W. H. Stockmayer, and A. A. Jones, *J. Polym. Sci., Polym. Phys. Ed.* **15**, 1347 (1977), and references cited therein.
(2) T.-P. Liao, Y. Okamoto, and H. Morawetz, *Macromolecules*, **12**, 535 (1979).
(3) M. A. Cochran, L. H. Dunbar, A. M. North, and R. A. Pethrick, *J. Chem. Soc., Faraday Trans. 2*, **70**, 215 (1974).
(4) T. F. Schatzki, *J. Polym. Sci.*, **57**, 496 (1962); *Polym. Prepr., Am. Chem. Soc., Div. Polym. Chem.*, **6**, 646 (1965).
(5) L. Monnerie and F. Gëny, *J. Chim. Phys. Phys.-Chim. Biol.*, **66**, 1691 (1969).
(6) J. C. Keck, *Discuss. Faraday Soc.*, **33**, 173 (1962).
(7) C. Bennett, *ACS Symp. Ser.*, **No. 46** (1977).
(8) J. Skolnick and E. Helfand, *J. Chem. Phys.*, to be published.
(9) J. H. Weiner and M. R. Pear, *Macromolecules*, **10**, 317 (1977).
(10) E. Helfand, *J. Chem. Phys.*, **69**, 1010 (1978). Equation 3.2 of that reference is corrected by eq III.4 of the present paper.
(11) M. Fixman, *J. Chem. Phys.*, **69**, 1527 (1978).
(12) M. R. Pear and J. H. Weiner, *J. Chem. Phys.*, **71**, 212 (1979).
(13) (a) R. M. Levy, M. Karplus, and J. A. McCammon, *Chem. Phys. Lett.*, to be published; (b) G. T. Evans and D. C. Knauss, to be published.
(14) D. Chandler, Report of the Workshop on Stochastic Molecular Dynamics, July 1978, National Resource for Computations in Chemistry, Lawrence Berkeley Laboratory, Berkeley, CA.
(15) J. P. Ryckaert and A. Bellemans, *Chem. Phys. Lett.*, **30**, 123 (1975); *Faraday Discuss.*, to be published.
(16) T. A. Weber, *J. Chem. Phys.*, **69**, 2347 (1978); **70**, 4277 (1979).
(17) T. A. Weber and E. Helfand, *J. Chem. Phys.*, **71**, 4760 (1979).
(18) E. Helfand, Z. R. Wasserman, and T. A. Weber, *J. Chem. Phys.*, **70**, 2016 (1979).
(19) R. Zbinden, "Infrared Spectroscopy of High Polymers", Academic Press, New York, 1964.
(20) M. Fixman, *Proc. Natl. Acad. Sci. U.S.A.*, **71**, 3050 (1974); E. Helfand, *J. Chem. Phys.*, **71**, 5000 (1979), and references cited therein.
(21) E. Helfand, *Bell Syst. Tech. J.*, **58**, 2289 (1979).
(22) N. R. Mann, R. E. Schafer, and N. D. Singpurwalla, "Methods for Statistical Analysis of Reliability and Life Data", Wiley, New York, 1974.
(23) H. A. Kramers, *Physica (Utrecht)*, **7**, 284 (1940).
(24) E. Helfand, *J. Chem. Phys.*, **54**, 4651 (1971).

Conformational Properties of Poly(L-proline) and Poly(γ-hydroxy-L-proline). 2. Salt-Induced Isomerization‡

Leo Mandelkern,* Donald S. Clark, and James J. Dechter

Department of Chemistry and Institute of Molecular Biophysics, Florida State University, Tallahassee, Florida 32306.

Received September 28, 1979

ABSTRACT: The quantitative determination of the extent of imide bond isomerization in poly(L-proline) and poly(γ-hydroxy-L-proline) in aqueous salt solutions is reported. The results are quite different for the two polymers, and this major conformational change does not correlate with the measured intrinsic viscosity as a function of salt concentration. A generalized salt binding mechanism is proposed which allows for the repopulation of the conformational energy state in the vicinity of $\Psi = -50°$. A major difference between the two chains is caused by the intramolecular hydroxyl group interaction which makes cis isomerization energetically unfavorable and also retards the population of the other trans state. When these factors are taken into account, very good agreement is obtained between the intrinsic viscosity and the total salt induced conformational change. These results also allow for a general understanding of salt effects in polypeptides which do not undergo isomerization about the amide group.

In the previous paper of this series, we have shown that in pure solvents the all-trans poly(L-proline), poly(Pro), and poly(γ-hydroxy-L-proline), poly(Hyp), chains possess conformational energy minima in the vicinity of $\Psi = 160°$ as well as at $\Psi = -50°$.[1] Both of these conformational energy states need to be populated to explain the characteristic ratios of the polymers in the different solvents. In addition it was found that, while a small fraction of the residues of both polymers are in the cis configuration in D_2O,[2,3] this configuration is absent for poly(Pro) in trifluoroethanol.[1]

Certain classes of salts, in aqueous solutions of polypeptides and polyimides, cause major changes in optical properties, such as the optical rotatory dispersion and circular dichroism, and in the chain conformation, as is reflected in hydrodynamic properties.[4,5] Although these salts affect all classes of polypeptides, polyimides, and the globular and fibrous proteins in this manner, the mechanism of their action has not as yet been universally demonstrated. However, Torchia and Bovey[6] and Dorman et al.[7] have demonstrated the presence of cis imide bonds in concentrated, aqueous salt solutions of poly(Pro) by both 220 MHz ^1H NMR and 15 and 25 MHz ^{13}C NMR. The detailed functional relation between the salt concentration, or activity, and the extent of isomerization has not, how-

‡ It is our pleasure and privilege to dedicate this paper to Professor Flory on the occasion of his 70th birthday celebration. His scientific accomplishments and incisive contributions to all aspects of polymer science need not be amplified by us. However, we take the opportunity on this occasion to wish this gentleman and scholar many more years of pioneering and exciting contributions to the science which he has pioneered and loves so dearly.

0024-9297/80/2213-0533$01.00/0